Structure and Properties of the Nickel(III) Oxide Family: $LnSr_5Ni_3O_{11}$ (Ln = Y, Dy, Ho, Er, and Tm)

M. James,[†,‡] J. P. Attfield,*[,†] and J. Rodriguez-Carvajal[§]

Department of Chemistry, University of Cambridge, Lensfield Road, Cambridge, CB2 1EW, U.K.; the Interdisciplinary Research Centre in Superconductivity, University of Cambridge, Madingley Road, Cambridge, CB3 0HE, U.K.; and the Laboratoire Léon Brillouin (CEA), CE-Saclay, F-91151, Gif-sur-Yvette, France

Received December 1, 1994. Revised Manuscript Received May 11, 1995[⊗]

Tetragonal K_2NiF_4 type phases $LnSr_5Ni_3O_{11}$ have been prepared for Ln = Dy, Ho, Er, and Tm. They are isostructural with previously reported $YSr_5Ni_3O_{11}$. Thermogravimetric analysis indicates that these phases are stoichiometric nickel(III) oxides. Rietveld refinement using X-ray and neutron powder diffraction data confirms that the Ln^{3+} and Sr^{2+} ions are disordered over the same lattice sites. Local structural features were investigated for $YSr_5Ni_3O_{11}$ using Sr and Y K edge EXAFS, and the total oxygen coordination number about the Y site, 7.7(3), was found to be lower than that of the Sr site, 8.6(3). Magnetic susceptibility data for these $LnSr_5Ni_3O_{11}$ phases show Curie–Weiss paramagnetic behavior between 6 and 300 K.

Introduction

Many mixed oxides of the type A_2BO_4 (A = lanthanide or alkaline earth, B = transition metal) crystallize with the tetragonal K_2NiF_4 (T-type) structure (Figure 1), composed of alternating perovskite (ABO_3) and rock-salt (AO) layers. This places the larger A ions in 9-fold coordination, forming double layers between octahedrally coordinated B ions. BO_6 octahedra share corners in the *ab* plane forming a two-dimensional array of B–O–B bonds, which give these compounds quasi two-dimensional magnetic and electrical properties.[1–4]

The structural, magnetic and electronic properties of $Ln_{2-x}Sr_xNiO_{4-\delta}$ solid solutions have been studied extensively for Ln = La[5–7] and Nd,[8,9] and the $Pr_{2-x}Sr_xNiO_{4-\delta}$ ($0 \le x \le 1.0$) and $Sm_{2-x}Sr_xNiO_{4-\delta}$ ($0.5 \le x \le 1.0$) solid solutions and $GdSrNiO_4$ have also been reported.[10] As part of a study of any solid solutions formed by the smaller lanthanides, we previously showed that in the $Y_{2-x}Sr_xNiO_{4-\delta}$ system, a single phase was produced only for one composition ($x = 1.67$), corresponding to a stoichiometric K_2NiF_4-type defect phase $YSr_5Ni_3O_{11}$.[11] This paper reports further results for $YSr_5Ni_3O_{11}$ and the preparation of isostructural phases $LnSr_5Ni_3O_{11}$ (Ln = Dy, Ho, Er, Tm).

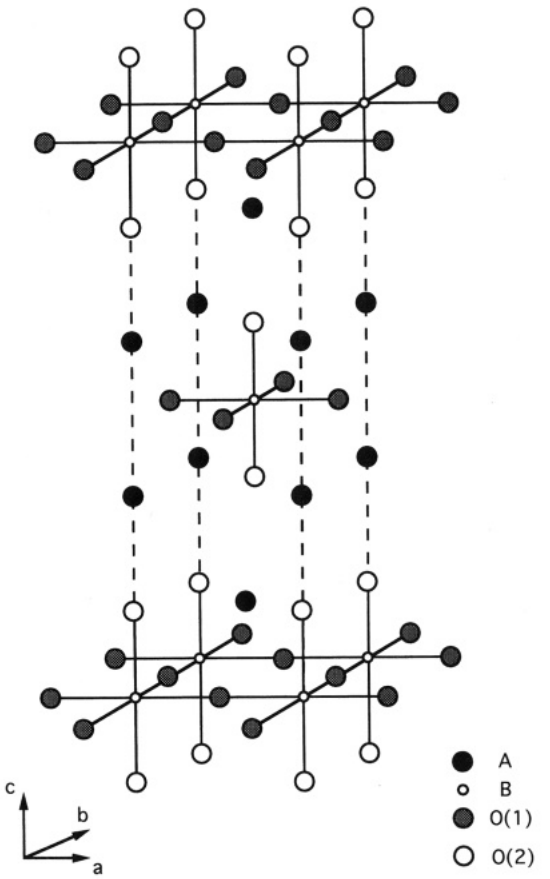

Figure 1. Crystal structure of A_2BO_4 with the tetragonal K_2NiF_4 structure type.

† Department of Chemistry, University of Cambridge, Lensfield Road, Cambridge, CB2 1EW, U.K., and Interdisciplinary Research Centre in Superconductivity, University of Cambridge, Madingley Road, Cambridge, CB3 0HE, U.K.

‡ New address: Lucas Heights Research Laboratories, Menai, NSW 2234, Australia.

§ Laboratoire Léon Brillouin (CEA), CE-Saclay, F-91151, Gif-sur-Yvette, France.

* To whom correspondence is to be addressed.

⊗ Abstract published in *Advance ACS Abstracts,* June 15, 1995.

(1) Bassat, J. M.; Odier, P.; Gervais, F. *Phys. Rev. B* **1987**, *35*, 7126.
(2) Buttery, D. J.; Honig, J. M.; Rao, C. N. R. *J. Solid State Chem.* **1986**, *64*, 287.
(3) Rao, C. N. R.; Buttery, D. J.; Otsuka, N.; Ganguly, P.; Harrison, H. R.; Sandberg, C. J.; Honig, J. M. *J. Solid State Chem.* **1984**, *51*, 266.
(4) Buttery, D. J.; Honig, J. M. *J. Solid State Chem.* **1988**, *72*, 38.
(5) Gopalakrishnan, J.; Colsmann G.; Reuter, B. *J. Solid State Chem.* **1977**, *22*, 145.
(6) Takeda, Y.; Kanno, R.; Sakano, M.; Yamamoto, O.; Takano, M.; Bando, Y; Akinaga, H.; Takita, K.; Goodenough, J. B. *Mater. Res. Bull.* **1990**, *25*, 293.
(7) Sreedhar, K.; Rao, C. N. *Mater. Res. Bull.* **1990**, *25*, 1235.
(8) Arbuckle, B. W.; Ramanujachary, K. V.; Zhang, Z.; Greenblatt, M. *J. Solid State Chem.* **1990**, *88*, 278.
(9) Takeda, Y.; Nishijima, M.; Imanishi, N.; Kanno, R.; Yamamoto O.; Takano, M. *J. Solid State Chem.* **1992**, *96*, 72.
(10) Chen, S. C.; Ramanujachary, K. V.; Greenblatt, M. *J. Solid State Chem.* **1993**, *105*, 444.
(11) James, M.; Attfield, J. P. *J. Solid State Chem.* **1993**, *105*, 287.

0897-4756/95/2807-1448$09.00/0

Experimental Section

Sample Preparation. Polycrystalline 1 g samples with bulk composition $LnSr_5Ni_3O_{11}$ (Ln = Tb, Dy, Ho, Er, Tm, Yb) were synthesized in the same manner as $YSr_5Ni_3O_{11}$.[11] The materials used were spectroscopic grade powders of strontium carbonate, nickel nitrate hexahydrate, and the lanthanide oxides Ln_2O_3 or Tb_4O_7. Prior to weighing, the lanthanide oxides were preheated to 1000 °C in air to decompose any carbonate material to the oxide. The powders were dissolved in dilute nitric acid, and an intimate mixture of the metal oxides was formed via the decomposition of a citric acid/ethylene glycol gel. The residues were pelleted and sintered in a tube furnace at 1100 °C under flowing oxygen for several days with frequent regrinding and repelleting until no further reaction was evident by powder X-ray diffraction. An additional ~10 g sample of $YSr_5Ni_3O_{11}$ was synthesized using the same technique for the neutron diffraction study.

Thermogravimetric Analysis. Thermogravimetric analyses of freshly annealed ~30 mg samples was carried out using a Stanton Redcroft STA 1500 simultaneous thermal analyzer. The sample was reduced under a 5% hydrogen in nitrogen mixture (flow-rate of 58 mL $min.^{-1}$), over the temperature range 15–900 °C at a heating rate of 10 °C $min.^{-1}$.

Powder Diffraction. Powder X-Ray diffraction profiles were recorded on a Philips PW1710 Diffractometer, utilizing Cu Kα radiation. Data of sufficient quality for structural refinement were collected over $13° \leq 2\Theta \leq 113°$, in 0.025° steps, with integration times of 12 s. The neutron diffraction profile for $YSr_5Ni_3O_{11}$ was collected on the D1A instrument at the Laboratoire Leon Brillouin, Saclay, France, using a wavelength of 1.9820(2) Å for $2\Theta = 15–149.5°$ in 0.05° steps. Rietveld refinements[12] were performed with the GSAS program,[13] using a refined background function.

Extended X-ray Absorption Fine Structure (EXAFS). EXAFS spectra for $YSr_5Ni_3O_{11}$ were collected in transmission mode at the Sr and Y K edges, using instrument 9.2 at the SERC Daresbury Laboratory Synchrotron Radiation Source, Warrington U.K. The sample was that used in the original X-ray diffraction study of this material.[11] Data for the Sr spectrum were collected over the energy range 15780–16970 eV (up to $k = 15.0$ cm^{-1}), while those for the Y spectrum were collected over the range 16790–18010 eV (up to $k = 16.0$ cm^{-1}). Both spectra had increments of 0.04 cm^{-1} between measurements and integration times of 10 s at each point. The EXAFS oscillations were extracted using the program EXBACK[14] and the program EXCURV92[14] was used to compare experimental data with calculated values based on our structural model.

Magnetic Susceptibility Measurements. Magnetic susceptibilities were measured using a Quantum Design SQUID magnetometer under an applied field of 3.0 T. Samples were cooled to 6 K in zero field and the magnetization was measured while warming to 300 K.

Results

The nominal composition $LnSr_5Ni_3O_{11}$ was prepared for Ln = Tb, Dy, Ho, Er, Tm, and Yb. The Tb sample contained a mixture of $Sr_5Ni_4O_{11}$,[15] SrO, and the perovskite $SrTbO_3$.[16] The Yb preparation also led to a mixture of phases, including the new phase $YbSr_3NiO_6$,[17] which adopts a rhombohedral K_4PtCl_6 type structure, Yb_2SrO_4, SrO, and NiO. The new MSr_3NiO_6 phase is formed by a number of cations (M = Tm, Yb, Lu, In, and Sc) and will be discussed elsewhere.[18] Single-phase $LnSr_5Ni_3O_{11}$ type samples were obtained for Ln = Dy, Ho, Er, and Tm, and their powder X-ray diffraction were indexed upon body-centered tetragonal unit cells. Typical d spacings and peak intensities, for $HoSr_5Ni_3O_{11}$, are given in Table 1.

Table 1. Indexed X-ray Diffraction Pattern of $HoSr_5Ni_3O_{11}$

(*hkl*)	*d* spacing (Å)	rel intensity
002	6.104	6
101	3.588	10
004	3.065	9
103	2.767	100
110	2.658	80
112	2.440	2
105	2.058	12
006	2.048	14
114	2.011	23
200	1.882	33
202	1.800	1
211	1.669	2
116	1.624	9
204	1.606	5
107	1.592	3
213	1.558	26
008	1.537	2
215	1.390	6
206	1.387	10
220/118	1.332	9

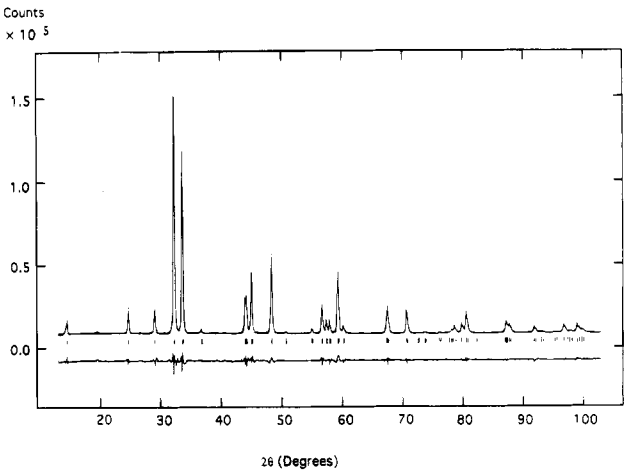

Figure 2. Observed (points), calculated (full line), and difference X-ray diffraction patterns for $HoSr_5Ni_3O_{11}$.

Slightly off-stoichiometric $Ln_{2-x}Sr_xNiO_{4-\delta}$ compositions led to the formation of secondary phases. $x < 1.67$ compositions led to additional phases of Ln_2SrO_4 and NiO, while Sr-rich $x > 1.67$ compositions gave SrO and NiO as secondary phases. The cell parameters of the K_2NiF_4-type phase varied only slightly with x. For example, in a multiphase sample of nominal composition $Er_{0.5}Sr_{1.5}NiO_{4-\delta}$ the values were $a = 3.770(1)$ Å and $c = 12.308(3)$ Å, and for nominal composition $Er_{0.2}Sr_{1.8}NiO_{4-\delta}$, $a = 3.774(1)$ Å and $c = 12.322(3)$ Å, indicating only a small range of solid solution around $x = 1.67$.

The powder X-ray diffraction patterns of the $LnSr_5Ni_3O_{11}$ phases were Rietveld-fitted using the model previously obtained for $YSr_5Ni_3O_{11}$.[11] A good fit was obtained using a pseudo-Voigt peak shape function and the peak width variation was found to be instrument limited. The resulting cell parameters are shown in Table 2; the refined atomic parameters did not differ

(12) Rietveld, H. M. *J. Appl. Cryst.* **1969**, *2*, 65.
(13) Larson, A. C.; Von Dreele, R. B. Los Alamos National Laboratory Report No. LA-UR-86-748 **1987**.
(14) Morrel, C.; Baines, J. T. M.; Campbell, J. C.; Diakun, C. P.; Dobson, B. R.; Greaves, G. N.; Hasnain, S. S. EXAFS Users' Manual, SERC Daresbury Laboratory,Warrington, U.K.
(15) Lee, J.; Holland, G. F. *J. Solid State Chem.* **1991**, *93*, 267.
(16) Paletla, E.; Hoppe, R. *Naturwissenschaften* **1966**, *53*, 611.
(17) James, M.; Attfield, J. P. *J. Mater. Chem.* **1994**, *4*, 575.
(18) James, M.; Attfield, J. P. Manuscript in preparation.

Table 2. Lattice Parameters (from Rietveld Refinement), Oxygen Content (from Thermogravimetric Analysis), and Magnetic Parameters for $LnSr_5Ni_3O_{11}$ (Ln = Y, Dy, Ho, Er, and Tm), with Esd's in Parentheses

Ln	Y[a]	Dy	Ho	Er	Tm
a (Å)	3.7762(1)	3.7820(1)	3.7755(1)	3.7742(1)	3.7755(1)
c (Å)	12.3011(4)	12.2919(4)	12.3206(3)	12.3269(5)	12.3146(3)
V (Å^3)	175.410(9)	175.818(9)	175.620(10)	175.592(10)	175.542(9)
oxygen content	11.01(4)	11.08(5)	11.07(5)	11.04(5)	11.37(6)
μ_{eff} per formula unit (μ_B)	1.0(1)	10.6(1)	10.6(1)	9.7(1)	8.2(1)
calcd $\mu_{eff}(Ln^{3+})$ (μ_B)[b]	0	10.7	10.6	9.6	7.6
Weiss θ parameter (K)	−10.8(1)	−7.7(1)	−11.7(1)	−10.9(1)	−9.2(1)

[a] Values taken from ref 11. [b] Calculated $\mu_{eff}(Ln^{3+}) = g_J(J[J+1])^{1/2}$ for ground state J, L, and S quantum numbers.

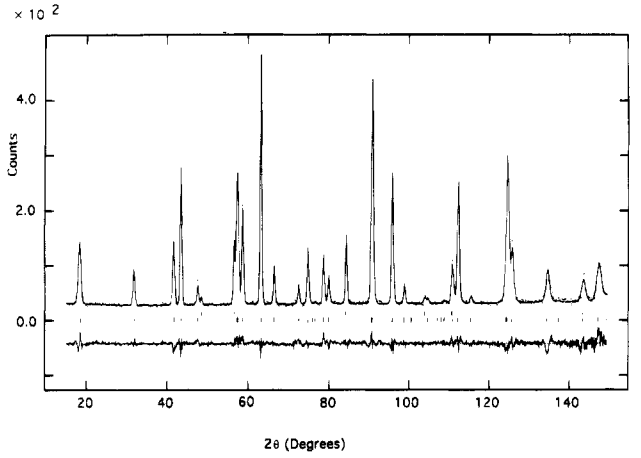

Figure 3. Observed (points), calculated (full line), and difference neutron diffraction patterns for $YSr_5Ni_3O_{11}$.

significantly from those of $YSr_5Ni_3O_{11}$. A typical fitted X-ray diffraction pattern, that of $HoSr_5Ni_3O_{11}$ (R_{WP} = 4.2%, R_P = 2.9%, and R_F = 3.9%), is shown in Figure 2.

The oxygen contents determined for the $LnSr_5Ni_3O_{11}$ phases by thermogravimetric reduction are displayed in Table 2. A typical plot of mass loss and the equivalent change in Ni oxidation state is shown for $DySr_5Ni_3O_{11}$ (Figure 3). Each one forms an intermediate phase indicated by a plateau at a mass-loss corresponding to reduction to Ni(I). These reduced phases $LnSr_5Ni_3O_8$ (Ln = Dy, Ho, Er, Tm,[19] and Y[20]) have recently been isolated and shown to adopt anion-defective Sr_2CuO_3 type structures.

To confirm the structure of the $LnSr_5Ni_3O_{11}$ phases, a Rietveld refinement of the $YSr_5Ni_3O_{11}$ structure using powder neutron diffraction data was performed. A small contribution from NiO was fitted as a second phase in the refinement. No evidence of a supercell due to Y/Sr or oxygen vacancy ordering was observed in these data. Constrained refinement of the distribution of 11 oxygen atoms/formula unit gave occupancies of 0.89(1) and 0.94 for the O(1) and O(2) sites (Figure 1), respectively, with values of R_{WP} = 7.1%, R_P = 6.2%, and R_F = 4.1%. Unconstrained refinement of the oxygen occupancies led to values of O(1) = 0.96(1) and O(2) = 1.00(1) with only marginally lower R factors; R_{WP} = 6.9%, R_P = 6.0%, and R_F = 3.9%. Final results for the constrained model are given in Table 3, and the observed, calculated, and difference neutron diffraction profiles are shown in Figure 4.

The inverse molar susceptibilities ($1/\chi_M$) of $LnSr_5Ni_3O_{11}$ (Ln = Dy, Ho, Er, and Tm) are shown in Figure 5. These data all show linear behavior that can be fitted by the Curie–Weiss equation $\chi_M = C\mu_{eff}^2/(T - \theta)$ and the derived molar effective magnetic moments (μ_{eff}) and Weiss θ parameters are given in Table 2.

Table 3. Profile and Structural Parameters from the Neutron Refinement of $YSr_5Ni_3O_{11}$ in Space Group *I4/mmm*, with Esd's in Parentheses

Cell Dimensions (Å)

a = 3.7790 (1) c = 12.3378 (4)

Profile Data

no. of reflns = 48 no. of points = 2990 no. of parameters = 25

R factors (%)

R_{WP} = 7.0 R_P = 6.1 R_F = 3.9

Atomic Parameters

atom	sym position	x	y	z	U_{iso} (Å^2)	site occupancy
Ni	2a	0	0	0	0.008(1)	1.0
Sr/Y	4e	0	0	0.3586(1)	0.009(1)	0.833/0.167
O(1)	4c	0.5	0	0	0.012(1)	0.89(1)
O(2)	4e	0	0	0.1598(5)	0.011(1)	0.94(1)

Bond Distances (Å)

Ni–O(1)	1.890(1)	Sr/Y–O(1)	2.572(1)
Ni–O(2)	1.972(2)	Sr/Y–O(2)	2.452(3)
mean Ni–O	1.921(1)	Sr/Y–O(2)′	2.682(3)
		mean Sr/Y–O	2.610(2)

Local order in $YSr_5Ni_3O_{11}$ was investigated by fitting the Sr and Y K edge EXAFS data. Initial values of the interatomic distances for each shell in the structural model were taken from the results of the Rietveld analysis of laboratory X-ray diffraction data for the same sample.[11] Initial values of coordination number were set to their fully occupied values; while the Debye–Waller factor for each shell was set to 0.01 Å^2. The distance and Debye–Waller parameters were refined in two blocks so as to avoid correlations. In the final stages, the coordination number of the first shell was refined in the same block as the Debye–Waller factors. Fourteen shells encompassing interatomic distances up to 6.5 Å and 86 backscattering atoms were used in the refinement of the Sr EXAFS model, and fifteen shells up to 6.3 Å and 85 atoms were used in the refinement of the Y model.

The ideal crystallographic Y/Sr site is nine-coordinate, neglecting vacancies, with contacts Y/Sr–O(2) 2.407(7) Å (×1), Y/Sr–O(1) 2.574(1) Å (×4), and Y/Sr–O(2) 2.681(1) Å (×4).[11] However, the short Y/Sr–O(2) contact could not be modeled separately as a stable shell, and so was combined with the Y/Sr–O(1) shell. The occupancy of this first shell was refined, in addition to the interatomic distances and Debye–Waller factors, as the crystallographic results showed that oxygen vacancies were predominantly at the O(1) sites. The fitted Sr and Y K edge k^3-weighted EXAFS spectra and their Fourier transforms are shown in Figure 6. Peaks in the

(19) James, M.; Attfield, J. P. *J. Chem. Soc., Chem. Commun.* **1994**, 1185.
(20) James, M.; Attfield, J. P. *Physica C* **1994**, *235*–240, 751.

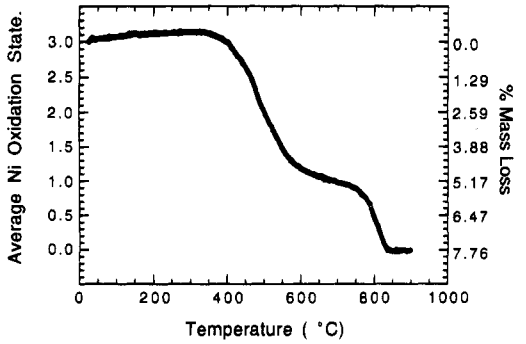

Figure 4. Percentage mass loss and the change in Ni oxidation state versus temperature for $DySr_5Ni_3O_{11}$ heated under 5% H_2 in N_2.

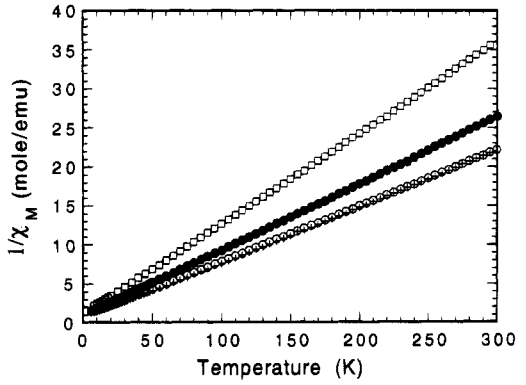

Figure 5. The inverse of the molar susceptibility ($1/\chi_M$) versus temperature for $LnSr_5Ni_3O_{11}$ (Ln = Dy, crosses; Ho, open circles; Er, closed circles; Tm, open squares). The Dy and Ho data coincide.

Fourier transforms below ~2 Å correspond to XANES features of the energy spectrum and have not been fitted in the refinements. The results of these refinements are summarised in Table 4.

Discussion

Our results show that $LnSr_5Ni_3O_{11}$ phases form for Ln = Y, Dy, Ho, Er, and Tm at 1100 °C under 1 bar of O_2. Yb is too small to stabilize this structure under these conditions, and Tb gives a multiphase mixture including the oxidized product $SrTbO_3$. The $LnSr_5Ni_3O_{11}$ phases are essentially stoichiometric, as off-stoichiometric $Ln_{2-x}Sr_xNiO_{4-\delta}$ starting compositions result in secondary phases. The cell parameters for the primary phase in the Ln = Er system indicate that the range of solid solution is no more than ±0.05 in x. Thermogravimetric reductions (Table 2) indicate that $LnSr_5Ni_3O_{11}$ phases are stoichiometric in oxygen and contain Ni^{3+}, except for Tm where the anomalous result may reflect small amounts of secondary phases, as this element is at the lower limit of the region of phase stability. (We have found that only Tm forms both $LnSr_5Ni_3O_{11}$ and $LnSr_3NiO_6$ type phases.) The thermogravimetric results also indicate that these phases may be reduced to analogous Ni(I) compounds, which have been isolated and are described elsewhere.[19,20] Stable Ni(I) oxides are unusual and have only previously been reported in $LaNiO_2$[21] and MNa_2NiO_2 (M = K, Rb).[22]

The compounds $LnSr_5Ni_3O_{11}$ (Ln = Y, Dy, Ho, Er, and Tm) all adopt the tetragonal K_2NiF_4-type structure. The cell parameters and volume (Table 2) decrease with decreasing Ln^{3+} radius. Disorder of the Ln and Sr atoms over the K sites is confirmed by the X-ray Rietveld refinements of the structures with Ln = Dy–Tm in which no Ln/Sr ordering is observed, although the contrast in Ln/Sr X-ray scattering factors is large. However, it has not been possible to refine the Ln/Sr ratio accurately, as there is some correlation between the total occupancy of this site and the overall scale factor. The Y/Sr ratio could also not be refined in the neutron study, as the neutron scattering lengths of Y (7.65 fm) and Sr (6.9 fm) are similar.

Our previous study of $YSr_5Ni_3O_{11}$ using X-ray diffraction data[11] revealed a level of oxygen vacancies consistent with the above stoichiometry, predominantly in the NiO_2 planes, and no evidence of cation or oxygen vacancy ordering was found. This feature is confirmed by our neutron diffraction study (of a different sample), but the constrained oxygen vacancy distribution is different as a significant level of vacancies is found in both the in-plane O(1) sites (11%) and the out-of-plane O(2) sites (6%). Unconstrained Rietveld refinement of the oxygen occupation factors in $YSr_5Ni_3O_{11}$ from our neutron diffraction data gives an unrealistically high oxygen content, corresponding to an average nickel oxidation state of +3.5, which is in conflict with the thermogravimetric analysis. This seems to result from correlations between the refined occupancies and Debye–Waller factors, which may reflect local disorder around the oxygen sites due to the size discrepancy between Sr^{2+} and Y^{3+}, as evidenced in the EXAFS study.

The $LnSr_5Ni_3O_{11}$ phases are unusual in having Ln^{3+} and Sr^{2+} disordered over the same lattice sites despite the ~20% disparity in their ionic radii. In most late lanthanide strontium oxides, the cations are ordered, with Sr^{2+} in a larger, more highly coordinated site. We have proposed that local adjustments of the A cation sites may take place to accommodate the different cations.[11] If we imagine $LnSr_5Ni_3O_{11}$ as resulting from the substitution of Ln^{3+} for Sr^{2+} in hypothetical "Sr_2NiO_4", with the formation of one oxygen vacancy adjacent to each Ln^{3+} in order to reduce the size of the coordination sphere, then compositions $Ln_ySr_{2-y}NiO_{4-y}$ result. The value of y is controlled by the nickel oxidation state (=4 − 3y) in order to maintain charge balance. The highest nickel oxidation state normally attainable under 1 bar of O_2 is +3, giving the observed value of $y = 1/3$, resulting in mean coordination numbers of ~8.5 for Sr^{2+} and ~7.5 for Ln^{3+}.

This hypothesis is confirmed by the Sr and Y K-edge EXAFS study of the local Sr and Y coordinations in $YSr_5Ni_3O_{11}$ (Table 4). A significant difference between the mean Sr–O and Y–O distances of 0.21 Å is observed, comparable to the difference between their ionic radii (0.23 Å).[23] The refined coordination numbers for Y (7.7) and Sr (8.6) are also in agreement with the proposed model, although this difference is only significant within twice its combined error as is typical for EXAFS refinements. The differences between the bond lengths and the coordination numbers of Sr and Y were found to be unchanged by any truncation or Fourier filtering of the EXAFS data. The average EXAFS Sr/Y

(21) Crespin, M.; Levitz, P.; Gatineau, L. *J. Chem. Soc., Faraday Trans. 2* **1983**, *79*, 1181.
(22) Burow, W.; Birx, J.; Bernhardt, F.; Hoppe, R. *Z. Anorg. Allg. Chem.* **1993**, *619*, 923.
(23) Shannon, R. D. *Acta Crystallogr. Sect. A* **1976**, *32*, 751.

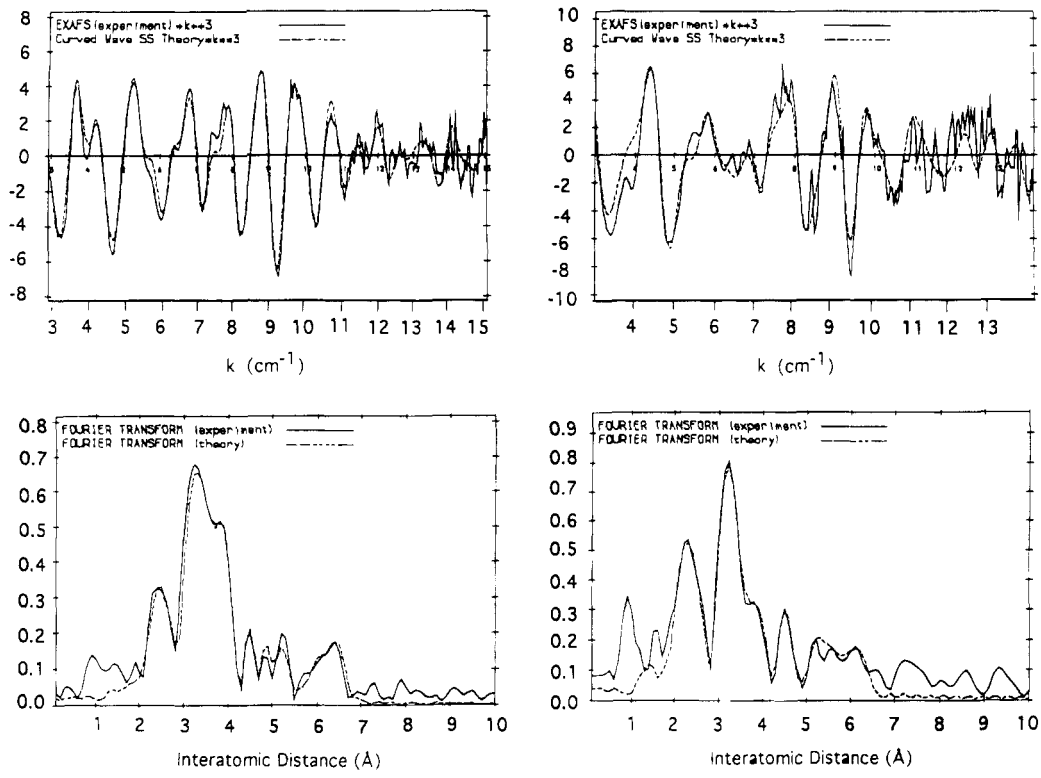

Figure 6. $YSr_5Ni_3O_{11}$ EXAFS spectra and their Fourier transforms for (a) the Sr K edge and (b) the Y K edge. Full lines indicate observed data, while broken lines indicate data calculated from the refined model.

Table 4. Interatomic Distances (Å) and Oxygen Coordination Numbers from the Y and Sr K-Edge EXAFS Study of $YSr_5Ni_3O_{11}$, with Esd's in Parentheses

M	first shell M–O (Å)	second shell M–O (Å)	total coordination no.[a]
Y	2.305(6)	2.446(9)	7.7(3)
Sr	2.509(6)	2.660(10)	8.6(3)
mean Y/Sr	2.475(6)	2.624(10)	8.4(3)
XRD Y/Sr	2.535(4)	2.681(1)	8.3(1)

[a] Coordination number varied for the first coordination shell and fixed at 4.0 for the second. [b] Results of the previous X-ray diffraction study of the same sample.[11]

coordination number of 8.4(3) corresponds to the structural average of $8^1/_3$.

Magnetic susceptibility measurements of $LnSr_5Ni_3O_{11}$ (Ln = Dy – Tm) reveal Curie–Weiss behavior down to 6 K. Little deviation from the Curie–Weiss law is found in any of the samples at low temperature, suggesting that the oxygen vacancies frustrate any long-range magnetic order. However, the negative values of the Weiss parameter (θ) suggest that antiferromagnetic Ni–O–Ni exchange occurs. The values of the effective magnetic moment approximate to those expected for Ln^{3+} and low spin Ni^{3+} ions, but for Ln = Dy–Tm the Ni^{3+} contribution cannot be estimated, due to small deviations of the lanthanide moments from their ideal values.

For $YSr_5Ni_3O_{11}$, the effective magnetic moment of 0.6 μ_B per Ni^{3+} is considerably lower than the spin-only value (1.73 μ_B).[24] This suggests that the paramagnetic moment is due to only ~10% of the Ni^{3+} spins within a secondary phase or a surface layer. The remaining spins may be antiferromagnetically coupled over the range 6–300 K due to very strong intraplane interactions with $|J/k| \gg 300$ K as are found in La_2CuO_4 and related copper oxides. The oxygen vacancies in the nickel oxide planes prevent long range magnetic order from occurring and result in variable range hopping semiconducting behavior, whereas the related $LnSrNiO_4$ phases (Ln = La, Nd) are metallic.[6–10]

(24) In a previous publication[11] the moment per Ni^{3+} was incorrectly stated to be 1.76 μ_B due to an erroneous factor of 10 in the susceptibility calculation. The true value is thus $1.76/\sqrt{10} \approx 0.6$.

Conclusions

A series of new nickel(III) oxides $LnSr_5Ni_3O_{11}$ (Ln = Y, Dy, Ho, Er and Tm), have been synthesized and characterized. Rietveld refinement using powder X-ray and neutron diffraction data show that these phases crystallise with the tetragonal K_2NiF_4 structure in space group $I4/mmm$. An EXAFS study at the Y and Sr K edges of $YSr_5Ni_3O_{11}$ supports the hypothesis that oxygen vacancies associated with the small Y^{3+} ions are important in stabilizing this structure. Susceptibility data from these materials show Curie–Weiss behavior, and do not reveal transitions to long-range magnetic order, although spin pairing within the nickel oxide planes is evidenced by a low value for the effective magnetic moment.

Acknowledgment. The authors wish to thank Drs. M. A. G. Aranda, M. D. Marcos, and T. Rayment for their assistance with collection and interpretation of the EXAFS data. M. J. is supported by the University of Sydney and Newman College, Melbourne University.

CM940534X